Detection of Motion Distorted Areas in Perfusion MRI of the Breast

Sebastian Schäfer, Klaus D. Tönnies

Department of Simulation and Graphics, University of Magdeburg
schaefer@isg.cs.uni-magdeburg.de

Abstract. Dynamic contrast-enhanced MRI of the breast (DCE-MRI) is widely used for detection and quantification purposes of breast cancer. The particular acquisition procedure of DCE-MRI over time leads to motion artifacts which distort analysis results. In this work we examine two criteria for a segmentation approach to separate areas affected by motion artifacts from properly perfused regions. By application of our approach to simulated perfusion data we showed that a homogeneity measure based on perfusion parameters achieves the best segmentation results with respect to the ground truth. This effect was confirmed when segmenting patient data.

1 Introduction

In North America and Europe, breast cancer is the most frequent mortal disease in women. Medical imaging techniques play an important role in diagnosis. In particular high-risk cases DCE-MRI of the breast allows a sophisticated analysis of lesion dynamics. A breast tumor leads to formation of new vessels, which is referred to as angiogenesis [1]. In DCE-MRI a contrast agent (CA) is intravenously injected and works as a tracer of perfusion. The angiogenetic activity leads to CA accumulations and allows for breast cancer detection through the calculation of perfusion parameters.

A current method to determine perfusion parameters for different lesions is to define regions with similar perfusion characteristics (Regions of Interest, ROI). Calculating an average over the ROI reduces the influence of noise. Many tools allow for manual ROI placement, although this carries the risk of missing important details of the data and is subject to inter- and intra-observer variability. We employ a method by Glaßer et al. [2] to automatically generate ROIs in DCE-MRI to derive perfusion parameters of tumorous tissue.

Motion artifacts which are based on patient motion during acquisition hamper the correct determination of perfusion parameters. They result in incorrect inter-voxel correspondences between images at different times. In the automatic region generation method, this results in smaller regions of homogeneously perfused tissue and produces new regions with mixed perfusion parameters.

To reduce the influence of motion a global registration approach can be applied (e.g. we use a method by Rueckert et al. [3]). It optimizes the voxel po-

sitions using mutual information as similarity measure and a continuous deformation function (e.g. B-Splines). Hence, there exists a high conformance at the boundary between breast and background but in tumor regions within the breast it is less accurate. This is caused by the fact that entropy is high even for images in perfect registration because of change of CA concentration. This leads to a less well pronounced minimum for the registration criterion. Other approaches have tried to compensate for this. Melbourne et al. [4] analyze principal components of the currently best registered two images and optimize them in an iterative process. If periodic motion is present though, it will be propagated in the principal components. Xiaohua et al. [5] merge the process of segmentation and registration to incorporate knowledge of regional anatomy to align different images, but no reliable evaluation for non-rigid registration results is provided.

Although many attempts have been conducted, a perfect registration is still hard to achieve. Thus, remaining motion artifacts have to be identified by abnormal perfusion parameter characteristics. The goal of this study is to examine which criteria are well suited for this purpose.

2 Materials and Methods

For the investigation presented here we use a region merging segmentation approach [2] and tested two different merging criteria. These criteria are defined such that the algorithm produces homogeneous regions in terms of a defined correlation threshold. The first criterion employs the raw intensity values which have been measured at particular time steps. As regions contain multiple voxels, image values are averaged over each time measurement when merged with other regions. The vector V_1 containing relevant information for a region R is

$$V_1(R) = (R_0, ..., R_{n-1})^T \tag{1}$$

where n is the number of time points measured in the dataset. It is assumed that similar perfusion characteristics lead to similar measured values in two different regions. It should be noted that image artifacts, particularly noise, motion and partial volume effects will be directly represented in the vector data. Hence, they will influence the calculation of similarity of regions.

The second criterion uses general properties of the averaged perfusion time course of a region. The curve properties are employed as indicators for diagnostic purposes as well [6]. The feature vector V_2 in ((2)) incorporates three parameters which are calculated from the perfusion time curve.

$$V_2(R) = (S_{up}(R), S_{down}(R), RE_m(R))^T \tag{2}$$

$$S_{up}(R) = \left(\frac{R_{\lfloor n/2 \rfloor} - R_0}{R_0} \right) \tag{3}$$

$$S_{down}(R) = \left(\frac{R_{\lfloor n/2 \rfloor} - R_{n-1}}{R_{n-1}} \right) \tag{4}$$

$$RE_m(R) = \left(\frac{\max(R_0, ..., R_{n-1}) - R_0}{R_0} \right) \tag{5}$$

Table 1. Comparison of criterion V_1 and V_2 using different statistical measures. The best performing measures (SP, SE, REL, NPV) of either V_1 or V_2 are printed bold.

	criterion V_1				criterion V_2			
displacement	SP	SE	REL	NPV	SP	SE	REL	NPV
1 pixel	**0.912**	0.878	**0.979**	0.612	0.876	**0.905**	0.970	**0.675**
2 pixel	0.983	0.851	0.980	0.872	**0.986**	**0.934**	**0.986**	**0.932**
3 pixel	0.972	0.827	0.965	0.855	**0.974**	**0.876**	**0.969**	**0.895**

The upslope (Eq. (3)) characterizes the early enhancement intensity, the downslope (Eq. (4)) shows the washout of CA from the tissue and the relative enhancement in ((5)) represents the maximum enhancement of the curve. R denotes the current region and n the number of measured time steps.

Two different experiments have been accomplished to test both similarity criteria for their ability to distinguish between normal and motion distorted areas in the image. The first experiment is performed with simulated data, showing a lesion with two differently enhancing regions. Artificial motion displacement is added with different magnitude and relative enhancement curves (REC) of segmented regions are evaluated. This shows the effects solely caused by motion artifacts. The second experiment is performed with patient data (manually registered and unregistered) to see whether similar effects as in the first experiment can be observed.

3 Results

In this section we describe the outcome of the experiments previously outlined. The different rows in Fig. 1 show the results of the segmentation of the simulated dataset. The extent of motion influence increases from 0 pixels to up to 3 pixels offset per time step. The 1 pixel and 2 pixel offset is a linear shift whereas the 3 pixel image is generated by a rotation.

Tab. 1 shows the detection performance for both criteria of the simulated images. Therefore all segments have been manually classified as regions representing motion artifacts (M) and regions not influenced by motion (P). The specificity (SP) expresses the likelihood of a segment being classified as P and belonging to class P. The sensitivity (SE) expresses the likelihood of a segment being classified as M and belonging to class M. The relevance (REL) expresses the proportion of segments correctly classified as P and all segments classified as P. The negative predictive value (NPV) expresses the proportion of segments correctly classified as M and all segments classified as M.

For the second experiment a ROI of a DCE-MRI data set showing contrast enhancement in tumorous tissue has been manually registered by an expert. Both the registered and unregistered image have been segmented with the proposed approach. Results are shown for the parameter-based criterion V_2 (Fig. 2), because it achieves better results in the first experiment.

4 Discussion

Both similarity criteria are able to segment the two differently perfused areas of the simulated data (first row of Fig. 1). However, using criterion V_2 results in much fewer regions (avg. of 20) compared to criterion V_1 (avg. of 40). This fact enables a better distinction between regions showing correct perfusion characteristics and those influenced by motion (see column 3 and 5 in Fig. 1). In Tab. 1 SE and the NPV characterize the performance of segmenting motion distorted areas. The criterion using V_2 leads to a better performance, especially when a stronger influence of motion is present. V_2 also performs better for the segmentation of correctly perfused areas (SP and REL). Therefore this criterion should be preferred. The second experiment analyzes patient data. The regional REC of the manually registered image are very similar and indicate normal perfusion

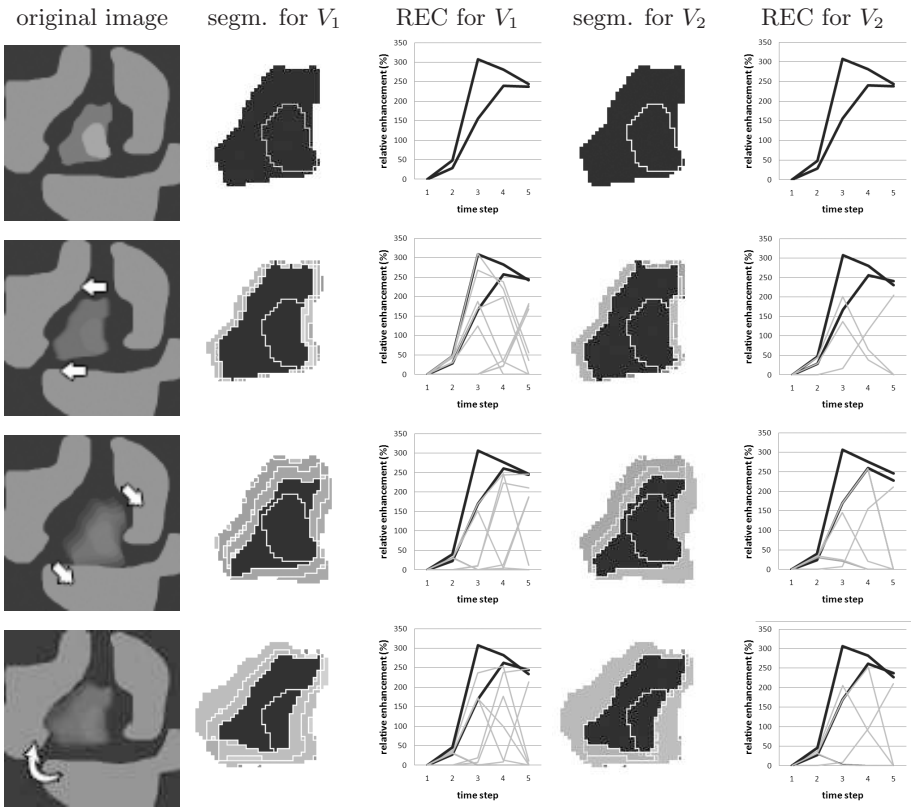

Fig. 1. Each row depicts the results of simulated perfusion data with different extent of motion influence. The first column shows the image itself, the second shows the segmentation result for criterion V_1 and the third column the enhancement curves for the segmented regions. Column 4 and 5 show the results for criterion V_2 likewise. The two region curves showing the true perfusion characteristics are printed bold and black.

Fig. 2. Segmentation results for manually registered (a) and unregistered (b) patient data is shown. (c) and (d) present the REC of (a)/(b) for regions bigger than 5 voxels.

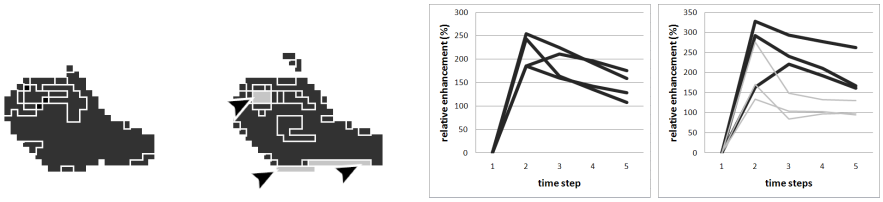

(a) (b) (c) (d)

characteristics (Fig. 2). The unregistered image leads to formation of new regions near the boundary (black mark) which show different time courses (dotted curves) than the correctly perfused parts. This implies that similar effects than in the first experiment can be observed in patient data.

Further steps will be focused on the motion correction to DCE-MRI. The proposed method can then be used to evaluate and conduct the correction process although more experiments have to be performed with patient data. As the parameter-based model yields promising results, the use of a more sophisticated model might be useful. Though, we plan to implement a pharmacokinetic model to measure the plausibility of derived REC to automatically distinguish between realistic perfusion parameters and those influenced by artifacts.

Acknowledgement. We thank Uta Preim for providing the medical data. This work has been funded by DFG (research grant no. TO166/13-1).

References

1. Kuhl CK. The current status of breast MR imaging, Part I. Radiology. 2007;244(2):356–78.
2. Glaßer S, Schäfer S, Oeltze S, et al. A visual analytics approach to diagnosis of breast DCE-MRI data. Proc VMV. 2009; p. 351–62.
3. Rueckert D, Sonoda L, Hayes C, et al. Nonrigid registration using free-form deformations. IEEE Trans Med Imaging. 1999;18(8):712–21.
4. Melbourne A, Atkinson D, White M, et al. Registration of dynamic contrast-enhanced MRI using a progressive principal component registration (PPCR). Phys Med Biol. 2007;52(17):5147–56.
5. Xiaohua C, Brady M, Rueckert D. Simultaneous segmentation and registration for medical image. In: Proc MICCAI; 2004. p. 663–70.
6. Preim B, Oeltze S, Mlejnek M, et al. Survey of the visual exploration and analysis of perfusion data. IEEE Trans Vis Comput Graph. 2009;15(2):205–20.